SYSTEMATIC STUDIES OF JET QUENCHING IN HOT NUCLEAR MATTER

A Senior Scholars Thesis

by

ANDREA DELGADO

Submitted to the Office of Undergraduate Research
Texas A&M University
in partial fulfillment of the requirements for the designation as

UNDERGRADUATE RESEARCH SCHOLAR

April 2011

Major: Physics

SYSTEMATIC STUDIES OF JET QUENCHING IN HOT NUCLEAR MATTER

A Senior Scholars Thesis

by

ANDREA DELGADO

Submitted to the Office of Undergraduate Research
Texas A&M University
in partial fulfillment of the requirements for the designation as

UNDERGRADUATE RESEARCH SCHOLAR

Approved by:

Research Advisor: Rainer J. Fries
Director for Honors and Undergraduate Research: Sumana Datta

April 2011

Major: Physics

ABSTRACT

Systematic Studies of Jet Quenching in Hot Nuclear Matter. (April 2011)

Andrea Delgado
Department of Physics and Astronomy
Texas A&M University

Research Advisor: Dr. Rainer J. Fries
Department of Physics and Astronomy

The early universe was filled with a primordial form of matter called Quark Gluon Plasma that only exists at extremely high temperatures and densities, many times hotter than the core temperature of suns. By colliding heavy nuclei at top energies at machines like the Relativistic Heavy Ion Collider (RHIC) and the Large Hadron Collider (LHC) we can create and investigate tiny bubbles of Quark Gluon Plasma for very short periods of time before they cool and decay. We can use so-called QCD jets i.e. highly energetic quarks and gluons to penetrate and probe these artificially created Quark Gluon Plasma bubbles by comparing them with jets created in vacuum in control experiments. This is a wonderful tool to study properties of this exotic form of matter. We conduct a systematic study of the functional relationship between the so-called jet quenching strength $\hat{q}$ and the plasma entropy density s. Our main goal is to explore the possibility of enhanced energy loss when the plasma temperature is close to the phase transition, temperature between the Quark Gluon Plasma and ordinary nuclear matter. We will simulate jets in Quark Gluon Plasma for a variety of colliding nuclei and collision energies. Existing

experimental data will lead to constraints on the relationship between the plasma entropy density and the quenching strength.

We were able to qualitatively confirm the results by Liao and Shuryak [8] who postulated an enhancement of $\hat{q}$ around the phase transition. For Pb+Pb collisions at the LHC we can show that such scenario leads to predictions of relatively small energy loss and small elliptic flow which can be compared to future experimental data.

NOMENCLATURE

RHIC	Relativistic Heavy Ion Collider
LHC	Large Hadron Collider
QCD	Quantum Chromodynamics
QGP	Quark Gluon Plasma
T	Temperature
T_c	Critical Temperature
s	Entropy Density
$\hat{q}$	Transport Coefficient
E	Energy Loss Rate
P	Proton
Au	Gold Nucleus
$\vec{b}$	Impact Parameter
N_{coll}	Number of Binary Nucleon-nucleon Collisions
N_{part}	Number of Participating Nucleons
σ_{inel}	Inelastic Nucleon-nucleon Cross Section
$\sqrt{S_{NN}}$	Beam Energy
R_{AA}	Nuclear Modification Factor
v_2	Azimuthal Anisotropy
c	Quenching Strength
λ	Suppression of Quenching at Large Entropy
w(s)	Profile Function
ρ_{part}	Density of Binary Collisions

ρ_{part}	Density of Participant Nucleons

TABLE OF CONTENTS

LIST OF FIGURES

FIGURE Page

LIST OF TABLES

CHAPTER I

INTRODUCTION

Nuclear matter

For many years, it was believed that the atom was the most elemental form of matter; now we know that the atom is indeed made up of protons, electrons and neutrons, and, at the same time, protons and neutrons are made up of quarks and gluons. Scientists at the Relativistic Heavy Ion Collider (RHIC) and the Large Hadron Collider (LHC) are trying to explore the properties of these particles by colliding heavy nuclei traveling at nearly the speed of light. When this happens, the nuclear matter heats up, and protons and neutrons melt into their quark and gluon constituents. This hot state of nuclear matter is called Quark Gluon Plasma (QGP). The importance of these experiments lies in the belief that QGP was the original form of matter filling the universe after the Big Bang, before it cooled down and formed protons and neutrons. The melting of protons and neutrons into quarks and gluons happens at temperatures $T \sim 10^{12}$ K, many thousand times the temperature in the core of the sun. We are able to produce these ultra-hot temperatures at RHIC and LHC and hence study tiny bubbles of QGP (also called fireballs) for a very small fraction of a second.

The standard model of elementary particles

The standard model describes three of the four fundamental interactions: electromagnetism, the weak and the strong nuclear force. The strong force is described by the Theory of Quantum Chromodynamics (QCD). In this model there are two sets of particles: fermions which have half

---

This thesis follows the style of *Physical Review C.*

–integer spin and bosons that have whole-integer spin. The fermions can then be divided into quarks and leptons and are classified in three generations.

Quarks are elementary particles that have a spin of ½ that cannot be observed as free particles. Instead, quarks are bonding to other quarks via gluons -which are bosons- to form normal nuclear matter called hadrons. These particles are most commonly seen in nature as protons and neutrons. Hadrons make up the largest amount of particles that are created from heavy-ion collisions.

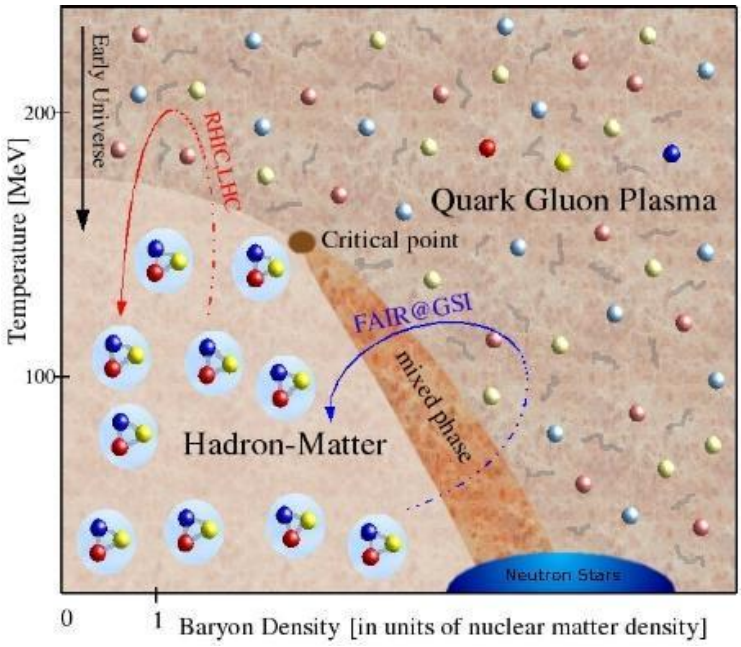

FIG. 1.1 Phase Diagram that shows nuclear matter phase transitions as a function of Temperature and Baryon Density. Baryon Density is measured in units of normal nuclear matter density ρ_0, which can be approximated from the size of the nucleus. We can see that we can achieve the phase transition from hadronic matter to a deconfined state by either increasing the temperature to around 170 MeV or by increasing the Baryon density. 170 MeV~1.972 x 10^{12} K.

Quark gluon plasma

Interactions between quarks and gluons (which are also called partons) can be thought of as analogous to the electromagnetic force between electrically charged particles. In order to be subject to the strong force particles need to carry a "color" charge, the equivalent of an electric charge for the strong force. Hadrons are color neutral particles. The main difference between strong forces and electromagnetic forces is the relationship between strength and distance; while the strength of the electromagnetic force decreases with increasing distance, the strength of the strong force increases with increasing distance. This leads to a unique phenomenon called confinement; quarks and gluons cannot be separated from each other. There always have to be enough quarks and gluons grouped together to make a color neutral hadron. Confinement is the main reason why it has been so difficult to study quarks and gluons as free particles. There are two ways to break this confinement; we can either increase the temperature or the net baryon density (the difference of baryon and antibaryons produced) to make the transition between the hadronic phase and free quarks and gluons. This can be seen in the phase diagram of nuclear matter shown in Fig. 1. This phase diagram shows the form that nuclear matter takes as a function of temperature T and baryon density ρ_0. At low temperatures T~0 and a baryon density of about $\rho_0 = 0.16$ fm^3, we have ordinary nuclear matter as we can find it in atoms: quarks and gluons are bound in protons and neutrons which in turn form atomic nuclei. At temperatures of a few MeV or higher nuclei might break, but quarks and gluons stay confined inside hadrons. Only at a critical temperature T_c of about 170 MeV a phase transition or crossover to QGP occurs. Experiments at RHIC (indicated by the red trajectory in Fig. 1) precisely explore the region around the critical temperature [1,2].

Jet quenching

Sometimes in collisions of nuclei two partons can collide at very high energy. In that case they do not become part of the QGP bubble (i.e. they do not thermalize), but the pair flies off in opposite directions with the speed of light. They still have to traverse the surrounding quark gluon medium. Some of them are absorbed by the medium; others lose a fraction of their energy and escape the plasma; when this happens, each parton fragments into a spray of hadrons which we call a (QCD) jet. This conversion into color neutral hadrons eventually has to happen because of the confinement property of the strong force. Colored partons cannot exist by themselves. The jets can be measured in particle detectors and studied in order to determine the properties of the original particle.

The energy loss of these high momentum quarks and gluons interacting with the hot and dense QGP can give us valuable information on the conditions inside the bubble and enables us to learn about QCD. These interactions result in changes in the jet fragmentation functions. This process is called jet quenching [3,4,5]. High energy nucleus-nucleus collisions allow us to change the scene of parton fragmentation from vacuum to a QCD medium, e.g. QGP, and to study the properties of this medium through modifications of the jet structure. This process is illustrated in FIG. 1.2.

An important observable to measure jet suppression is the Nuclear Modification Factor R_{AA}. It is a measure of the ratio of number of particles produced in nucleus+nucleus collisions N^{AA} to the number of particles produced in p+p collisions N^{PP}, scaled by the average number of binary nucleon-nucleon collisions N_{coll}. As a function of transverse momentum $\boldsymbol{p_T}$ of the particle it is defined as:

$$R_{AA} = \frac{dN^{AA}/dp_T}{N_{coll}dN^{pp}/dp_T} \tag{1.1}$$

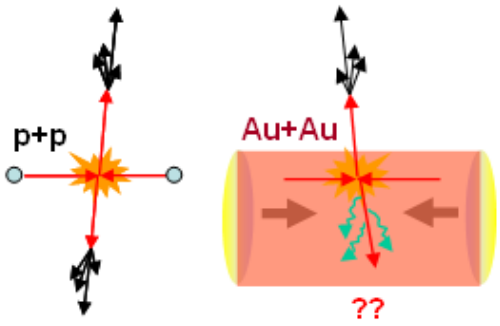

FIG. 1.2**.** Proton+Proton collision with two high energy partons colliding, leading to two jets coming out in opposite direction (Left). Gold+Gold collision with the same process. One jet is absorbed by the medium (in pink) and the other escapes (Right). The red lines indicate partons and black lines indicate sprays of hadrons.

The suppression of R_{AA} reflects the effect of high momentum partons losing energy or being absorbed. Fig. 3 shows experimental results on R_{AA} as a function of transverse momentum for several different hadron species in collisions of gold nuclei at 200 GeV. One can clearly observe a suppression ($R_{AA} < 1$) for hadrons from jets, e.g. high momentum ($\boldsymbol{p_T} > 5$ GeV/c) pions ($\boldsymbol{\pi^0}$).

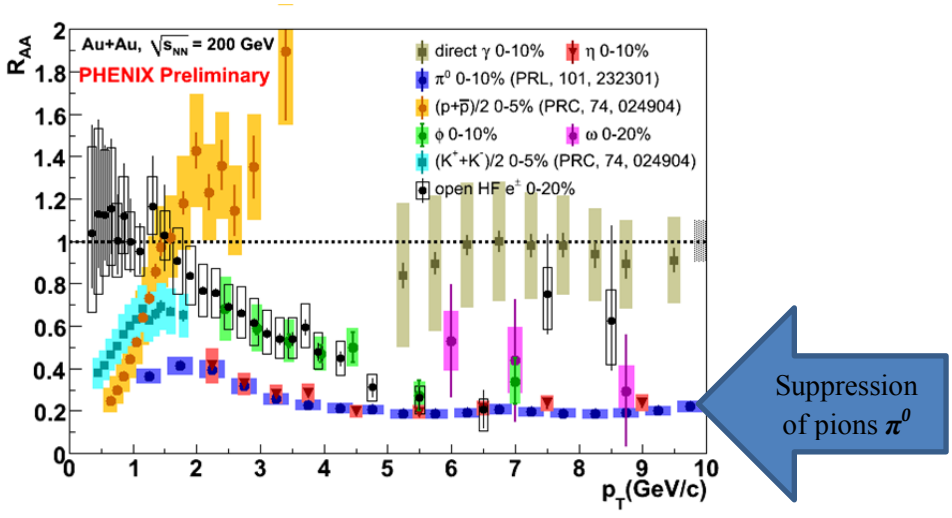

FIG. 1.3. Nuclear Modification Factor R_{AA} as a function of transverse momentum p_T for several particles in central an Au+Au collisions at 200 GeV. Data was collected by the PHENIX experiment at RHIC [6].

We will discuss more observables later in this work.

The rate of energy loss per path length, *dE/dx*, depends on a transport coefficient $\hat{q}$, $dE/dx \sim \hat{q}$ which describes a functional property of the QGP medium. The best way to describe a relativistic gas such as QGP is by terms of its entropy density $\boldsymbol{s}$. Therefore, it is usually assumed that $\hat{q}$ is proportional to *s*, $\hat{q} = cs$, where c is the parameter that measures the quenching strength per density of the medium in the region. Unfortunately, this relationship could not be proven mathematically.

Recently, it was hypothesized that $\hat{q}$ might break from this linear relation and be enhanced around the transition temperature T_c. This is motivated by other findings at RHIC which indicate that QGP is a strongly coupled liquid around T_c [7].

Indeed Liao and Shuryak have found that experimental data on jet quenching, in particular the azimuthal asymmetry v_2, favor enhanced energy loss around T_c [8]. They suggest a "shell" of strong quenching inside the fireball. Their scenario is schematically shown in Fig. 1.4.

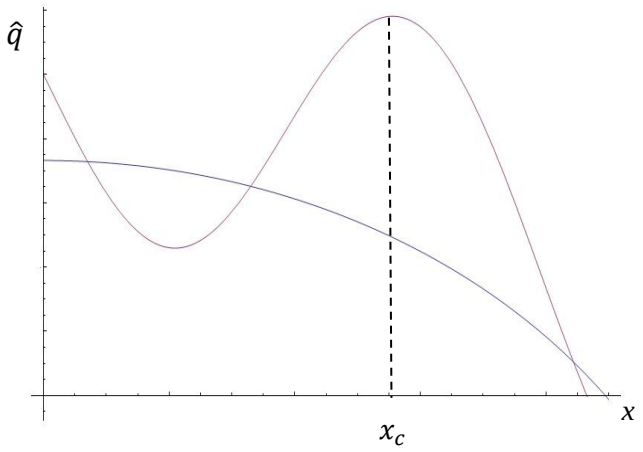

FIG. 1.4. Schematic scenario for shell-like quenching. We can see the linear dependence of $\hat{q}$ on *s* (in blue) and the shell-like dependence of Liao and Shuryak's model with the quenching strength peaking around T_c (in purple).

In this work we will systematically explore the functional dependence $\hat{q}(s)$ of energy loss on the local entropy density s. We will start with a test of the results of Liao and Shuryak. Then we check whether changing the size of the nuclei or the collision energy leads to better ways to distinguish normal energy loss from enhanced "shell-like" energy loss. In particular, we check whether the upcoming experiment at LHC can confirm or rule out this scenario.

CHAPTER II

METHODS

Relativistic Heavy – Ion Collisions are a unique tool to realize the QGP phase transition in a lab on earth. An important issue in this field is to pin down observables which could provide unambiguous information of the state of matter produced during a collision. Owing to the complexity of heavy-ion systems, it is likely that no single probe will yield definite conclusions and therefore it is important to investigate as many observables as possible and correlate their predictions. Likewise, we need to provide the system created in a nucleus-nucleus collision with the necessary conditions for QGP production and therefore we consider some geometric attributes such as the centrality.

The Glauber model

The Glauber model is used in relativistic heavy ion physics to calculate geometric quantities and spatial densities, which are usually the impact parameter *b,* given by the magnitude of the impact vector $\vec{b}$; the density ρ_{part} and total number N_{part} of participant nucleons; and the density ρ_{coll} and total number N_{coll} of binary nucleon-nucleon collisions (both given in terms of $\vec{b}$). As shown in FIG. 2.1, $\vec{b}$ is the impact vector in the transverse plane between the centers of two colliding nuclei A and B. Heavy-ion collisions with a small *b* and large overlap are called central collision. Likewise, collisions with large *b* and small overlap are called peripheral collisions. The more central a collision is, the more energy is deposited in the center of the collision and the more likely plasma production will be.

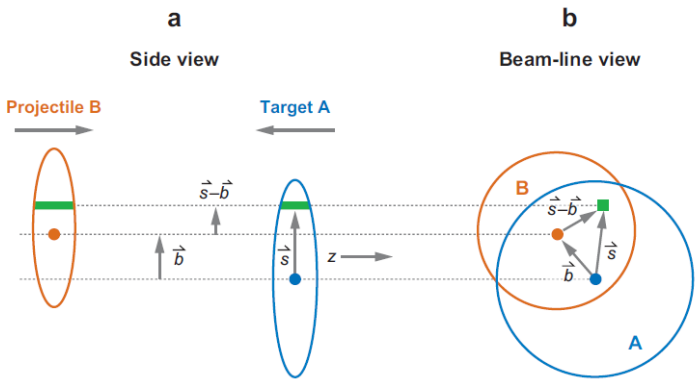

FIG. 2.1. Schematic representation of the optical Glauber model geometry, with transverse (a) and longitudinal (b) views [9].

Once an incident projectile nucleon undergoes a collision, the remnants of the collision can be treated as a projectile which continues to make collisions with other particles in the same direction of the projectile. The Glauber model is a geometrical model based on the assumption of a constant inelastic nucleon-nucleon cross section, σ_{inel}, for each subsequent collision. σ_{inel} has been measured in experiments and depends weakly on beam-energy $\sqrt{S_{NN}}$, as shown in Table 1.1[9,10].

Let us return to FIG. 2.1 and focus on a point $\vec{s}$ in the transverse plane. We take the origin of the coordinate system to be the center of nucleus A and $\vec{s}$ as the distance to a point inside the nucleus B.

A proton from nucleus B at position $\vec{s}$ would drill a cylindrical-shaped tube through nucleus A. We would be able to calculate the length of this tube by obtaining the thickness of the nucleus at that point. We define:

$$z_s = \sqrt{(R_A{}^2 - \vec{s}^2)} \tag{2.1}$$

TABLE 1.1. σ_{inel} dependence on beam energy $\sqrt{S_{NN}}$ [10].

$\sqrt{S_{NN}}$	σ_{inel}
20 GeV	32 mb
62.4 GeV	36 mb
200 GeV	42 mb
5.5 TeV	60 mb

The Nuclear Thickness Function $T_A(\vec{s})$ of nucleus A is the integral over the nuclear density over the longitudinal dimension,

$$T_A(\vec{s}) = \int dz \rho_A(\vec{s}, z) \tag{2.2}$$

We assume that nuclei are hard spheres with constant density ρ_0 inside:

$$\rho_A = \rho_0 \theta_R = \rho_0 \theta\left[(z^2 + \vec{s}^2) - {R_A}^2\right] \tag{2.3}$$

where ρ_0 is given by $3/4\pi {r_0}^3$ (r_0 is a parameter measured to be ~ 1.2 fm), and $R_A = r_0 A^{1/3}$ is the nuclear radius. We have that:

$$T_A(\vec{s}) = \rho_0 \int_{-z_s}^{+z_s} dz = 2\,\rho_0 \sqrt{({R_A}^2 - \vec{s}^2)} \tag{2.4}$$

During collision, the green tubes in FIG. 2.1 overlap. The interaction of these two rows of nucleons is sometimes referred to as row-on-row collisions. We can calculate the probability of a nucleon-nucleon collision at a given position in the transverse plane. Consider now a point

$(\overrightarrow{b_A}, z_A)$ in nucleus A and a point $(\overrightarrow{b_B}, z_B)$ in nucleus B with respect to the center of each nucleus. The probability for finding a nucleon inside a volume enclosed by $d^2b_A dz_A$ at a position $(\overrightarrow{b_A}, z_A)$ in nucleus A is:

$$\frac{\rho_A(\overrightarrow{b_A}, z_A)}{A} d^2\overrightarrow{b_A} dz_A \tag{2.5}$$

Which is normalized so that the integration over the volume gives unity and the we can define $\int d^3r\rho_A(\vec{r}) = A$. We follow the same procedure in Equation (2.5) for nucleus B. Now we can obtain the probability for one nucleon from A and one nucleon from B colliding at the same transverse position $\vec{s}$ by multiplying the individual probabilities, multiplying with the cross section and imposing that the positions overlap at $\vec{s} = \overrightarrow{b_A} = \vec{b} - \overrightarrow{b_B}$

$$dP_{AB}(\vec{b}) = \sigma_{inel} \frac{\rho_A(\overrightarrow{b_A}, z_A)}{A} d^2\overrightarrow{b_A} dz_A \frac{\rho_B(\overrightarrow{b_B}, z_B)}{B} d^2\overrightarrow{b_B} dz_B \delta(\vec{b} - \overrightarrow{b_A} - \overrightarrow{b_B}) \tag{2.6}$$

Integrating over Equation (2.6) and multiplying with the AB yields the total number of collisions:

$$N_{coll}(\vec{b}) = \sigma_{inel} T_{AB}(\vec{b}) = \sigma_{inel} \int d^2\overrightarrow{b_A} dz_A d^2\overrightarrow{b_B} dz_B \rho_A(\overrightarrow{b_A}, z_A)\, \rho_B(\overrightarrow{b_B}, z_B) \delta(\vec{b} - \overrightarrow{b_A} - \overrightarrow{b_B}) \tag{2.7}$$

We can carry out the integral over $\overrightarrow{b_B}$ by using the delta function and identifying $\overrightarrow{b_A}$with $\vec{s}$:

$$N_{coll}(\vec{b}) = \sigma_{inel} \int d^2\vec{s} dz_A dz_B \rho_A(\vec{s}, z_A)\, \rho_B(|\vec{b} - \vec{s}|, z_B) \tag{2.8}$$

Replacing $\int \rho_A(\vec{r}, z)dz$ with $T_A(r)$we have:

$$T_{AB}(\vec{b}) = \int d^2s T_A(\vec{s})\, T_B(|\vec{b} - \vec{s}|) \tag{2.9}$$

which is called the nuclear overlap function. The product of σ_{inel} and the nuclear overlap function gives the number of nucleon-nucleon collision as a function of impact parameter:

$$N_{coll}(\vec{b}) = \sigma_{inel} T_{AB}(\vec{b}) \quad (2.10)$$

In the same way, we can calculate the number of participants if $\vec{b}$ is given:

$$N_{part}(\vec{b}) = \int d^2s \left[T_A(\vec{s}) \left(1 - exp\left[-\sigma_{inel} T_B\left(\left|\vec{b} - \vec{s}\right|\right)\right]\right) + T_B\left(\left|\vec{b} - \vec{s}\right|\right)(1 - exp[-\sigma_{inel} T_A(\vec{s})]) \right] \quad (2.11)$$

where the term $1 - exp[-\sigma_{inel} T_A(\vec{s})]$ comes from the sum over the probability for a nucleon-nucleon collision in the interaction of a hadron with a nucleus [10].

In addition, by not taking the final integral over positions in (2.9) we obtain the density of binary collisions, ρ_{coll}:

$$\rho_{coll} = \sigma_{inel} T_A(\vec{s}) T_B\left(\left|\vec{b} - \vec{s}\right|\right) \quad (2.12)$$

In the same way:

$$\rho_{part} = \left[T_A(\vec{s}) (1 - \exp(-\sigma_{inel} T_B\left(\left|\vec{b} - \vec{s}\right|\right))) \right] + \left[T_B\left(\left|\vec{b} - \vec{s}\right|\right)(1 - \exp(-\sigma_{inel} T_A(\vec{s}))) \right] \quad (2.13)$$

During the project, I designed an Optical Glauber Model simulation program, written in C++ language, with the purpose of calculating densities of binary nucleon-nucleon collisions and densities of participating nucleons. The program receives a value for the impact parameter as input and at the same time allows the user to modify the atomic number and the value for σ_{inel}. It creates 42x42 grids in the xy-plane and then computes the values for ρ_{coll} and ρ_{part}, at each grid point.

Calculating initial jets

I used the code LOJET, a FORTRAN-written program that calculates the momentum distribution of initial jets before they lose energy, i.e. before they interact with the medium. It was originally created for calculating jets for p+p collisions but it is well suited to provide the initial momentum

distributions of jets in nucleus-nucleus collisions [11]. It can handle different center of mass energies and atomic masses of nuclei [12,13].

Energy loss calculations

As the leading effect of these interactions between jets and the medium, we can calculate the rate of energy loss $\Delta \boldsymbol{E}$ by the original quark or gluon in a jet. For a medium with length τ, *dE/dx* is given by the product of the length of the medium times the transport coefficient $\hat{q}$:

$$\frac{dE}{dx} = \tau\hat{q} \tag{2.14}$$

Where the transport coefficient measures the square of the momentum transferred to the parton over the mean free path of the parton:

$$\hat{q} = \frac{\mu^2}{\lambda} \tag{2.15}$$

If we integrate over the total path traveled by the parton we have that

$$\Delta E = \int d\tau(\tau)\hat{q} \tag{2.16}$$

This sLPM model is inspired by the Landau-Pomeranchuk-Migdal effect. Measuring $\hat{q}$ is a major goal of the heavy ion program. The simplest possible assumption at this point is that it is proportional to the local entropy density *s*, i.e.:

$$\hat{q} = cs \tag{2.17}$$

where $\boldsymbol{c}$ is a parameter that measures the quenching strength per entropy density around.

Although parton energy loss models explain the data from RHIC qualitatively, they have problems with some of the measured observables. In particular, calculations usually underestimate the azimuthal anisotropy $\boldsymbol{v_2}$.

Liao and Shuryak conducted a systematic study in 2009 exploring the relationship between *s* and the position of the parton inside the fireball. They concluded that data favors the existence of a layer-wise geometrical limit where quenching is not simply proportional to the entropy density *s* but peaks for *s* close to T_C. In their study, they divided the fireball into twenty-four layers to explore this feature. They generalized equation (2.14) by introducing a profile function *w(s)* such that the sLPM energy loss formula takes the form:

$$\Delta E = c \int d\tau(\tau - \tau_0) s w(s) \tag{2.18}$$

Note that *w(s)*=1 corresponds to the traditional case in (2.16).

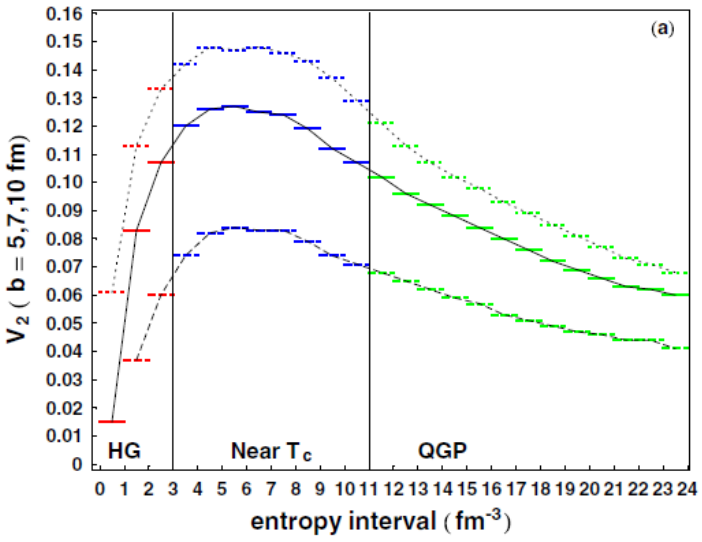

FIG. 2.2. The v_2 obtained by Liao and Shuryak for each entropy shell at b = 5 fm (dashed line), 7 fm (solid line), and 10 fm (dotted line) [8].

FIG. 2.2 shows the results by Liao and Shuryak which indicates that there is a region in the interval s=4-8 fm^{-3} where quenching peaks for all impact parameters. It corresponds to the vicinity of the QCD phase transition.

The proposed profile function which we will use here consists of a two-phase scenario model, with two parameters, one in the near-T_c region and the other for the QGP phase:

$$w(s) = [1\theta(s - {s_1}^c)\theta({s_2}^c - s) + \lambda\theta(s - {s_2}^c)] \quad (2.19)$$

We chose ${s_1}^c$ = 3/fm^{-3} and ${s_2}^c$ = 11/fm^{-3}as in [8]. Note that (2.19) means that for entropies below three there is no quenching, for entropies within the interval bracketed by ${s_1}^c$ and ${s_2}^c$ quenching is "normal", and for entropies above 11/fm^{-3} quenching is suppressed by a factor which we will fit to data. λ is the parameter that gives the suppression of quenching for large entropy[8].

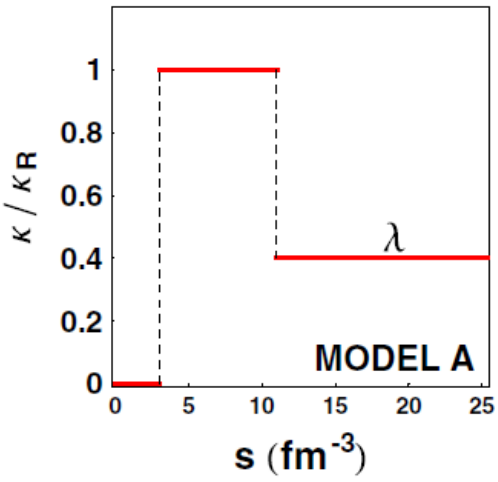

FIG. 2.3. Schematic demonstration of the quenching function[8].

Note that there are now two parameters in our energy loss calculations, λ and c. We will conduct a systematic study on the relationship between λ and c in order to find a useful pair to fit the results of our model calculations to experimental data.

Simulation program PPM

PPM (Propagation of Particles through a Medium) was developed at Texas A&M in order to simulate the energy loss of a quark and gluon jets in nuclear collision and to calculate a variety of observables [14].

The program reads an external file named parameters.dat, in which one can adjust several options such as:

- the hadron to be measured in experiment,
- energy loss model to be used (choosing from ASW, multiple and soft approximation, and sLPM),
- impact parameter,
- number of events,
- whether or not to use the profile function *w(s)*,
- the values for λ and c, etc.

The program calculates the momentum and spatial distribution of the initial jets by taking the density of binary collisions ρ_{coll} and the LOJET output. For a given entropy profile $s(\vec{r})$, being one of the energy loss models, PPM simulates the propagation of these jets through the fireball. $s(\vec{r})$ is derived from source or ρ_{part} as explained later. The main observable calculated by PPM is the hadron spectrum as a function of p_T and angle ψ in the transverse plane:

$$\frac{dN}{pdpdydd\psi} \tag{2.20}$$

used to calculate the other observables below.

Experimental observables

Nuclear modification factor, R_{AA}

The importance of R_{AA}, lies in the fact that one can explore the properties of the plasma by studying the interaction of these jets and the medium. As stated in Chapter I, R_{AA} measures the ratio of expected and experimental particle yield, which is then scaled by the number of binary collisions, equation (1.1).

Azimuthal anisotropy, v_2

At the beginning of a heavy ion collision, if non-central, the spatial distribution of the colliding matter resembles an ellipsoid due to incomplete overlap of the two colliding nuclei. Therefore, jets penetrating this almond-shaped fireball in different directions lose different amount of energy.

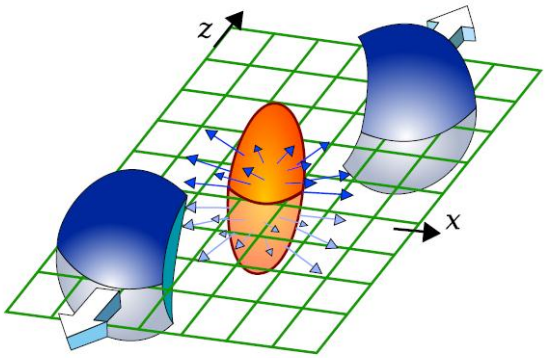

FIG. 2.4. The ellipsoidal shape of participant in non-central high energy nucleus-nucleus collisions.

We can calculate the eccentricity in momentum space in terms of the Second Fourier Coefficient:

$$v_2(p_T,\, b) \equiv \frac{\int_0^{2\pi} d\psi \, cos(2\emptyset)\left[\frac{d^2N}{dp_T d\psi}\right]}{\int_0^{2\pi} d\psi [d^2N/dp_T d\psi]} \tag{2.20}$$

CHAPTER III

RESULTS

This project aimed to simulate the propagation of jets through the fireball for a variety of system sizes, entropy densities, and beam energies in order to correlate these factors to suppression of such particles. We provided PPM with the initial spatial distribution by using ROPART and ROCOLL; and the initial momentum distribution provided by LOJET. By doing this, we were able to explore several systems such as those created by Cu+Cu, Au+Au, and Pb+Pb ion collisions. Moreover, we were able to investigate the suppression dependence on impact parameter b by simulating these collisions for centralities ranging from 0 to 60% .

As a first step we computed the initial momentum distribution for partons carrying transverse momentum between 1 and up to 200 GeV for different collisions by running LOJET. LOJET provides output as tables in intervals of 0.5 GeV. We used Mathematica to obtain fits of these tables with analytic functions. The shape we assume is of the form:

$$\frac{A(T-pT)^d}{(b+pT)^c}$$

with parameters a, b, and c provided by the parameterization while T is a kinematic cutoff given by the beam energy. The analytic formulas were then imported into PPM.

FIG. 3.1. shows some of our results for $dN/2\pi pTdpTdy$ from LOJET(blue dots), (taking only one out of five points for better comparison); versus the parameterized function (in red) obtained from Mathematica fits of those points. One can see that the overall quality of the fit is good.

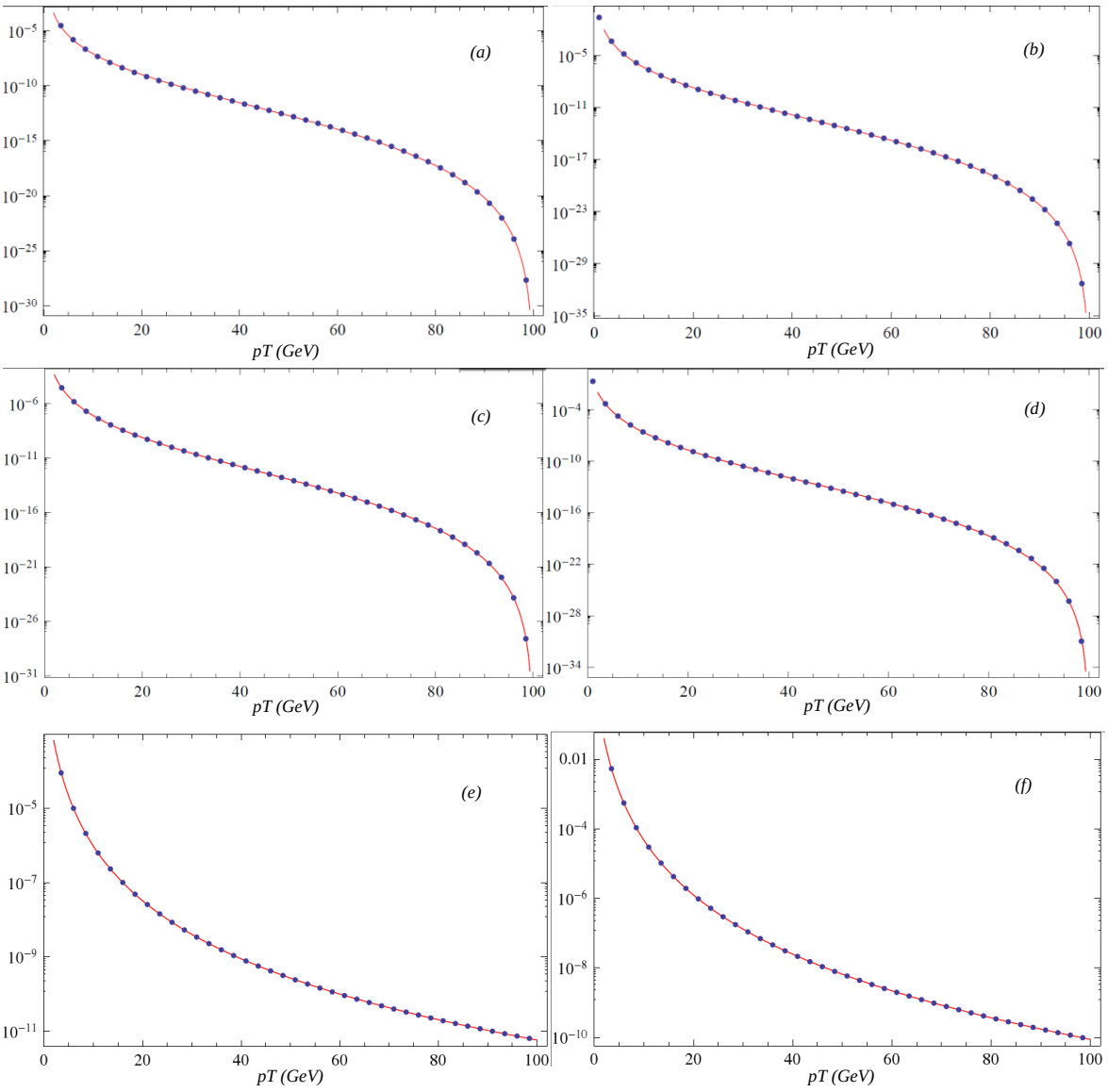

FIG. 3.1. Initial transverse momentum distribution for jets in Au+Au collisions [upper panels (a) and (b)], Cu+Cu jets [middle panels (c) and (d)], and Pb+Pb jets [lower panels (e) and (f)]. Left panels show up quarks [(a), (c), and (e)], and right panels show gluons [(b), (d), and (f)].

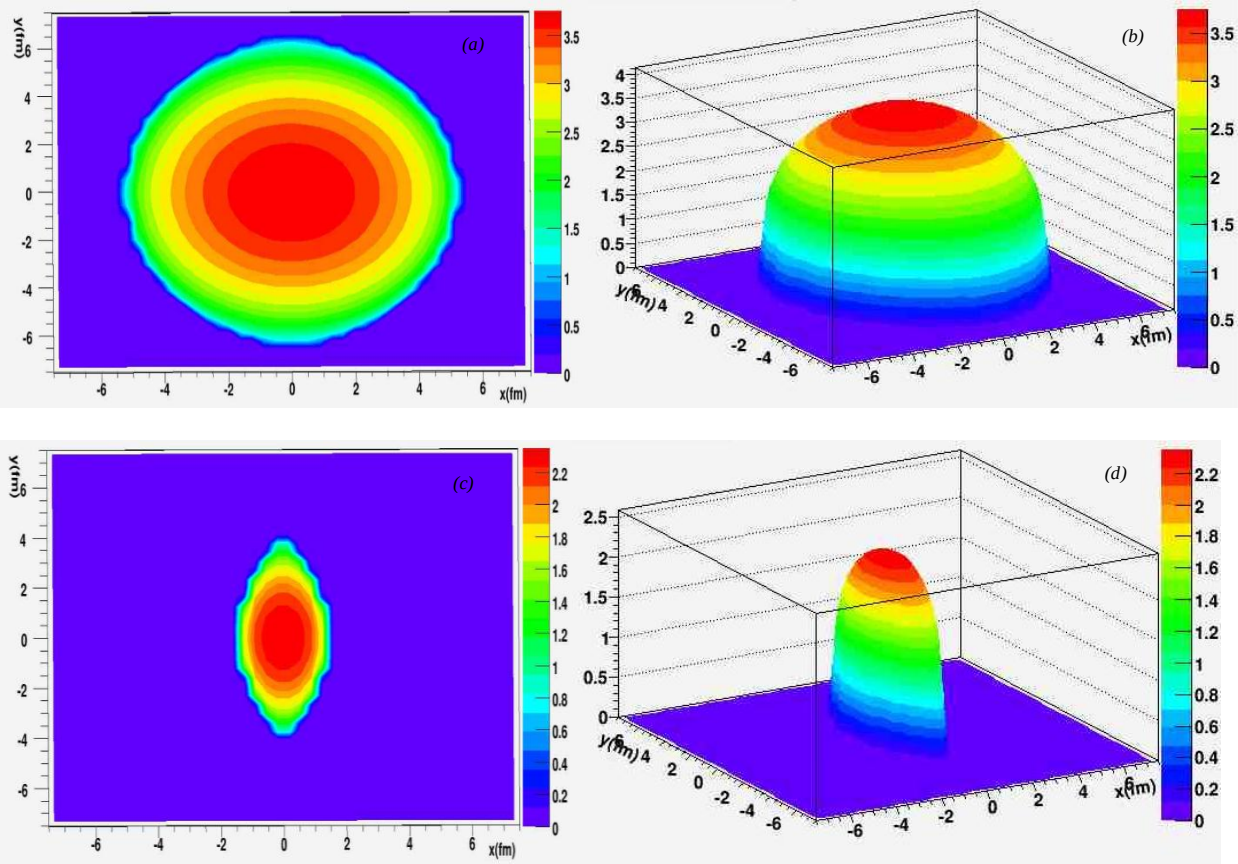

FIG. 3.2. Density of participants for Au+Au collisions at 200 GeV. Impact parameter 3.2 fm corresponding to most central bin (0-10%) displayed in (a) and (b); impact parameter 11.0 fm (50-60% centrality) in (c) and (d).

My code ROPART creates a n x n grid in the plane transverse to the beam axis, covering both colliding nuclei. The density of participants is calculated for each of these points as discussed in the previous chapter. We write out these results as a table. PPM reads in these values and calculates the number of participants per bin by multiplying by the bin size, i.e. the area associated with one point in the grid. We chose n=43 and the grid constant is 0.3665 fm.

FIG. 3.2 shows the density of binary collisions for Au+Au collision at 200 GeV for three different impact parameters. The impact parameter measures the distance between the centers of

two colliding nuclei and therefore a larger impact parameter implies a collision that is far from central. As expected, we observe a reduction in system size when going to the most central to peripheral impact parameter. For Au+Au collisions we chose the values of impact parameters that the PHENIX experiment gives as matching their centrality bins.

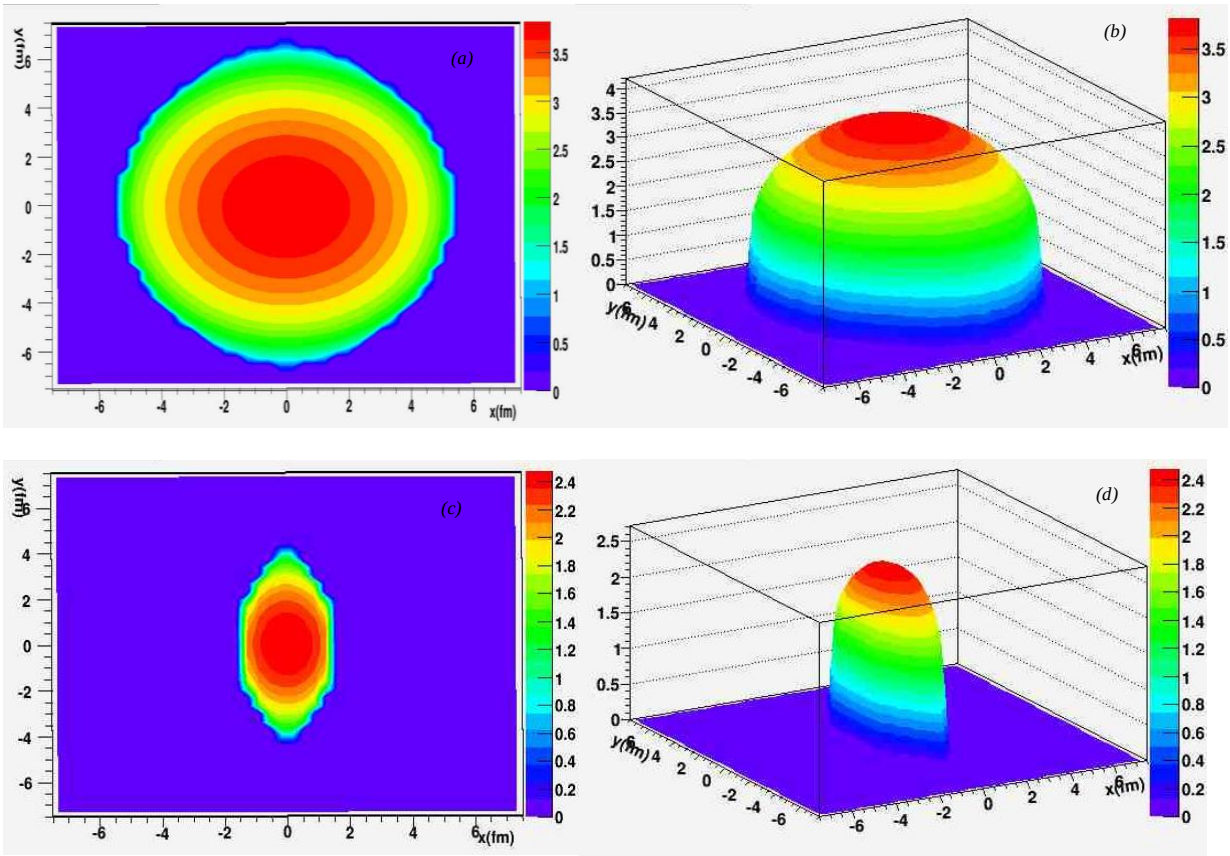

FIG. 5.3. Density of participants for Pb+Pb collision at 5.5 TeV. Impact parameter corresponding to most central bin (0-10%) displayed in (a) and (b); 50-60% centrality in (c) and (d).

When simulating a lead on lead system at the top LHC energy of 5.5 TeV we take the same impact parameter values that we used for the Au+Au system, that is, 3.2 fm, 7.4 fm, and 11 fm. We also used our Glauber Model to simulate Cu+Cu collisions at 200 GeV. For this system the PHENIX collaboration whose data we use does not provide a mapping of impact parameters onto experimental centrality bins. However they provide average numbers of total number of collisions and participants for each of their centrality bins. We choose a set of values for *b* so that the number of binary collisions, N_{coll}, and the number of participants N_{part}, from our calculations best fit their values calculated from a so called Glauber Monte Carlo (MC) calculation from. Table 3.1 compares our values with those of PHENIX for our choice of impact parameters. Note that there are minor deviations coming from the different Glauber models used.

TABLE 3.1. Optical Glauber and Glauber Monte Carlo (PHENIX experiment [15]) calculations for Cu+Cu colliding at 200 GeV beam energy.

Centrality	N_{coll} Optical Glauber	N_{coll} Glauber M.C.	N_{part} Optical Glauber	N_{part} Glauber M.C.
0-10%	189.9	182.7	88.1	98.2
20-30%	84.0	76.1	43.6	53.0
50-60%	19.2	16.7	12.4	16.2

We used ROCOLL to calculate the density of binary collisions for different collisions systems. Following the same criteria used for ROPART, results look similar for both densities. As expected, we observe a decrease in system size with decreasing impact parameter b as well as a higher probability for the parton to collide when located at the center of the collision system, i.e. x=0, y=0.

With the fireball and collision densities as well as the initial jet distributions in place we systematically studied v_2 and R_{AA} for 6 GeV neutral pions emerging from central Au+Au collisions at RHIC energies as functions of the quenching strength c and the suppression

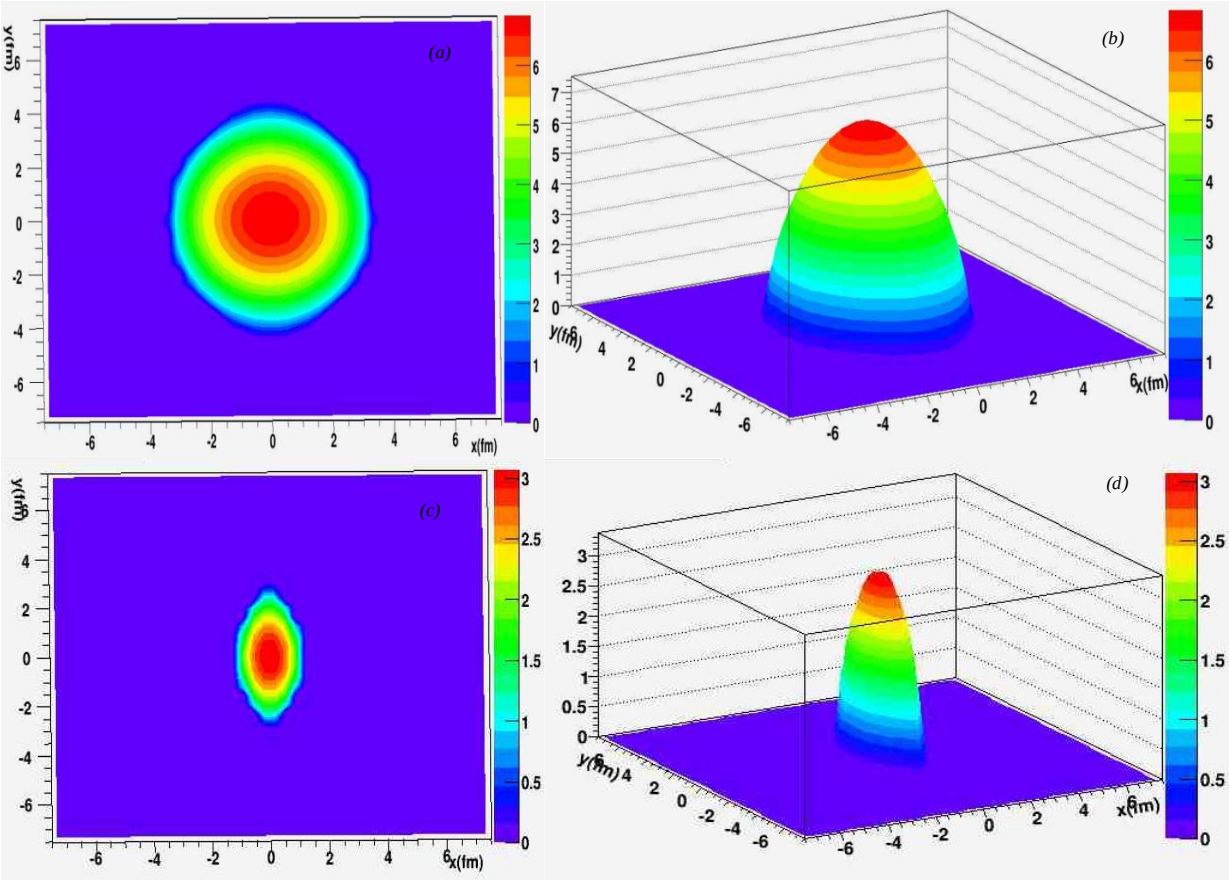

FIG. 3.4. Density of binary collisions for Cu+Cu colliding at 200 GeV. Impact parameter corresponding to most central bin (0-10%) displayed in (a) and (b); 50-60% centrality in (c) and (d).

parameter λ. The goal was to map out the behavior of v_2 and R_{AA} as a function of the absolute quenching strength and the enhancement 1/ λ around T_c. Results are shown in FIG. 3.5. As expected, for increasing c, i.e. overall increasing energy loss, jets are more suppressed, i.e. R_{AA} drops, and the azimuthal anisotropy is enhanced, i.e., v_2 increases. Decreasing λ from 1, i.e. reducing energy loss only in the high entropy density areas, leads to less suppression and higher R_{AA} which is also expected, but it slightly increases v_2 which is surprising. Note that this implies that if we decrease λ and at the same time increase c in order to keep R_{AA} constant, as we will describe in the next paragraph, we expect v_2 to increase even more, which was the claim by Liao and Shuryak. So already at this stage we qualitatively confirm the result by Liao and Shuryak that decreasing λ (increasing shell-like quenching) leads to a larger v_2.

Now we proceed to change λ and c at the same time such that the suppression R_{AA} stays the same and fits the data. We fit c for three different scenarios to Au+Au RHIC data for pions: (λ =1 [conventional], λ = 0.4 [Liao/Shuryak], λ = 0.01 [extreme shell scenario]). We find that the best values for c to fit R_{AA} from PHENIX are 0.09 GeVfm, 0.11 GeVfm, and 0.135 GeVfm, respectively. v_2 data from RHIC favors the lowest values of λ. Results for R_{AA} are shown in FIG. 3.6. We clearly see the results for all three pairs of (λ,c) fall on top of each other for each impact parameter which confirms the quality of each fitted value of c and the curves are also close to data. Now we look at the results of v_2 using all three pairs of (λ,c) on the left panels of FIG. 3.9. Even though the 3 scenarios (conventional, Liao/Shuryak and extreme shell) give the same R_{AA} for a given impact parameter, v_2 is clearly rising with decreasing λ for all impact parameters. It is largest for the extreme shell model where λ is almost zero, i.e. almost all the quenching is done in the critical region around T_c.

We then proceed to check how this result holds up at the much higher energy densities reached at LHC using the same three sets of parameters (λ,c) that fit R_{AA} at RHIC. In other words we make predictions for Pb+Pb collisions at 5.5 TeV at LHC.

We now look at the results obtained for LHC energies of 5.5 TeV displayed in FIG. 3.6. We observe more suppression with increasing λ and decreasing c at the same time, different from Au+Au results where curves would fall in top of each other. We can also say that suppression is higher for Pb+Pb collisions than it is for Au+Au collisions, since energy is greater and there is more mass involved in the collision

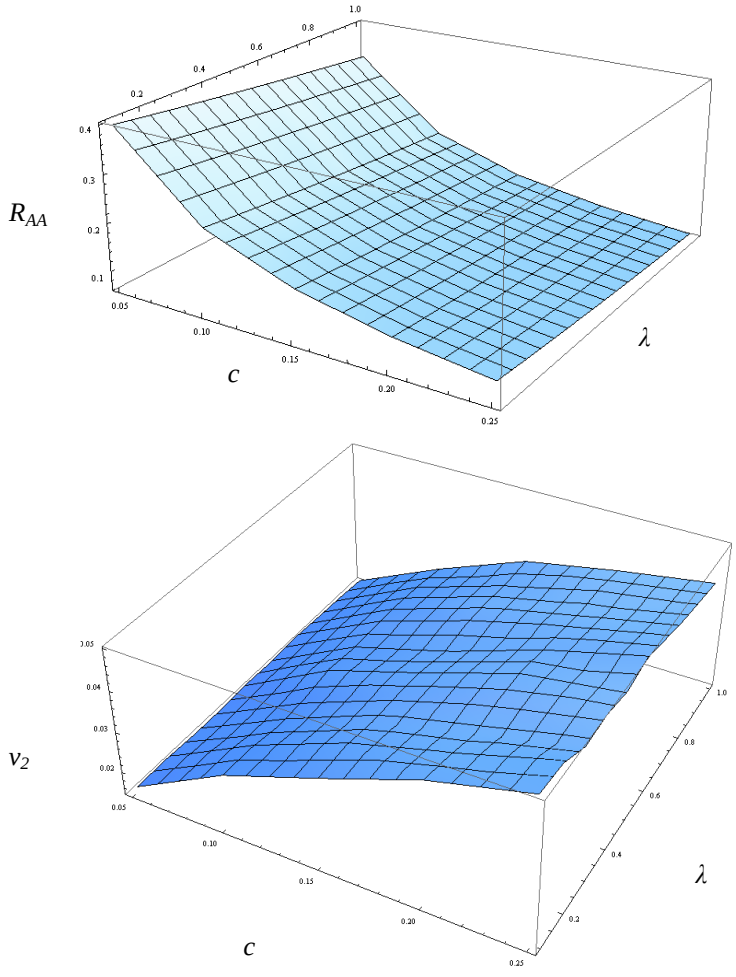

FIG. 3.5. Systematic study of dependence of v_2 and R_{AA} in quenching strength c and suppression parameter λ for 6 GeV pions in central Au+Au collisions at RHIC energies

LHC results for v_2 are another proof of the shell-like feature of the colliding system. We expect an increase in v_2 when going in the direction of decreasing λ. And for most systems we do indeed observe this, but for LHC we get exactly the opposite, v_2 increases in the direction of increasing λ.

We investigated the shell feature proposed by Liao and Shuryak by plotting the factor $(\tau - \tau_0)$ times the transport coefficient $\hat{q}$ as a function of τ for impact parameters b = 3.2 fm and 11.0 fm as shown in FIG. 3.8.The red curve corresponds to $\lambda = 1$ (conventional scenario) and we observe no shell feature as expected. By looking at b = 11.0 fm one can clearly see that the size of the shell is considerably reduced and it might explain the reversal in v_2 that we see in FIG. 3.9.

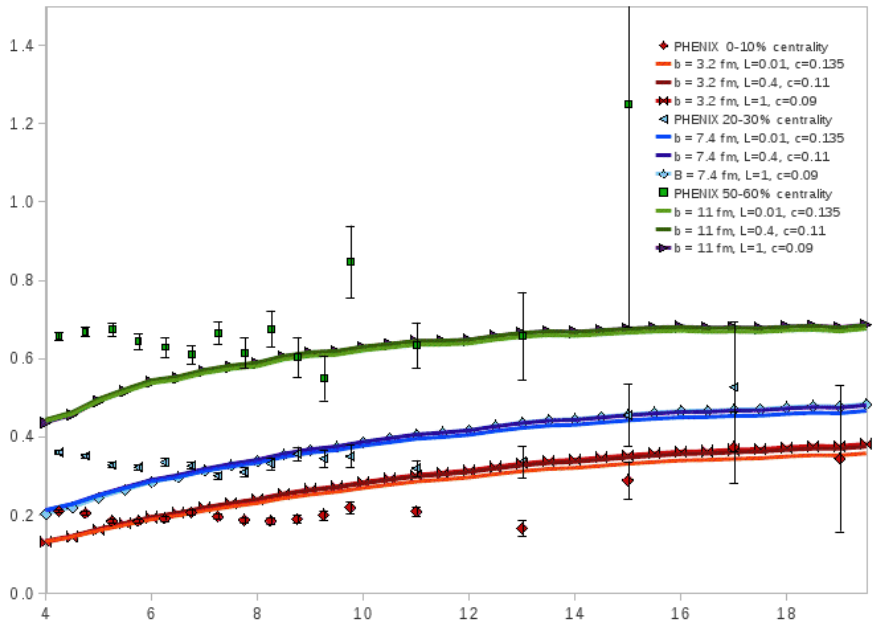

FIG. 3.6. Fitting of R_{AA} to PHENIX [3] experimental data for Au+Au collisions at 200 GeV.

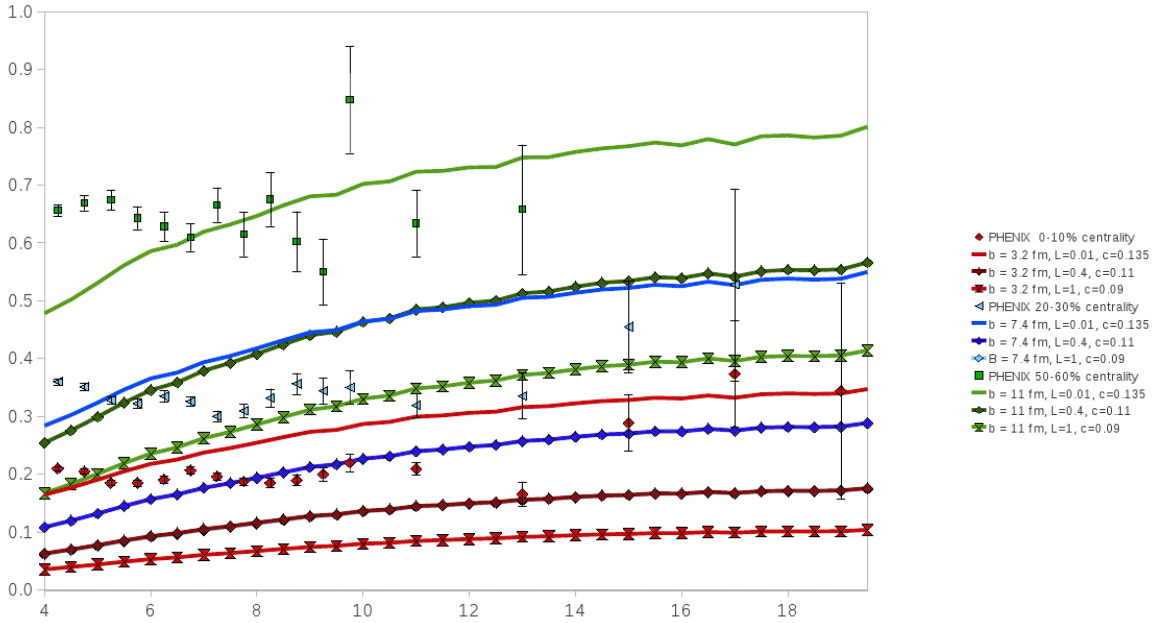

FIG. 3.7. R_{AA} results for Pb+Pb collisions at 5.5 TeV using the same parameters c and λ as for RHIC.

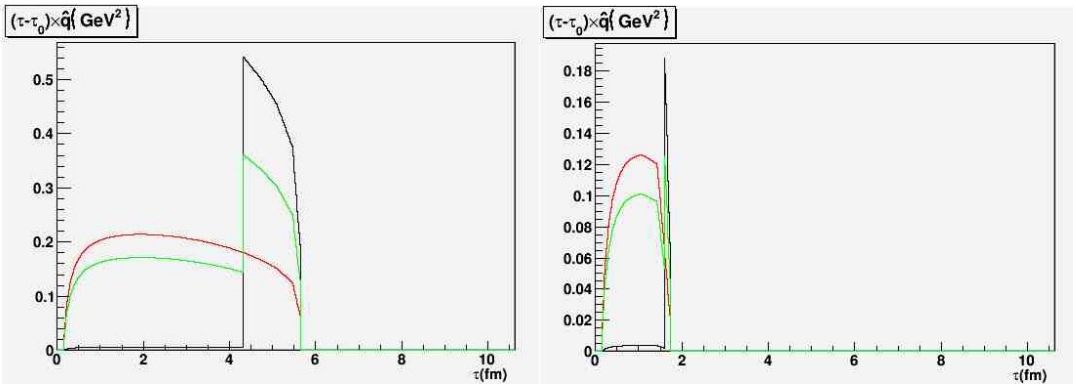

FIG. 3.8. Shell feature for Pb+Pb collisions at 5.5 TeV when plotting the factor $(\tau - \tau_0)$ times the transport coefficient $\hat{q}$ as a function of τ. Impact parameters b = 3.2 fm (left) and 11.0 fm displayed.

RHIC Energy LHC Energy

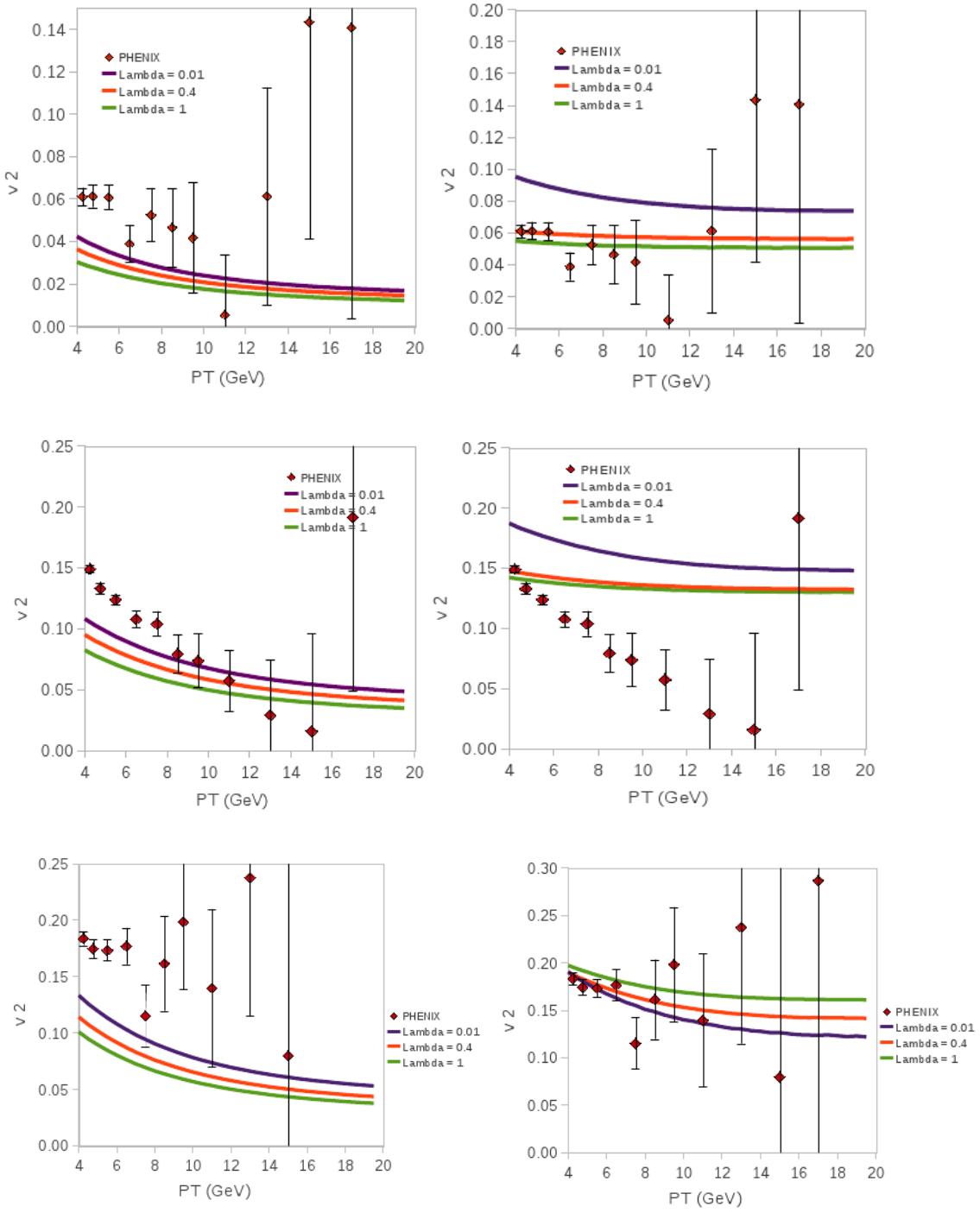

FIG. 3.9. v_2 results for energies at RHIC and LHC. Impact parameters 3.2 fm, 7.4 fm, and 11 fm shown in decreasing row order.

After we had satisfactorily fitted R_{AA} to experimental data for Au+Au collisions at 200 GeV and made predictions for LHC, the next step on the project was to simulate Cu+Cu collisions at 200 GeV with the same parameters c and λ. Results showed an underestimation for R_{AA} when comparing to PHENIX experimental data.

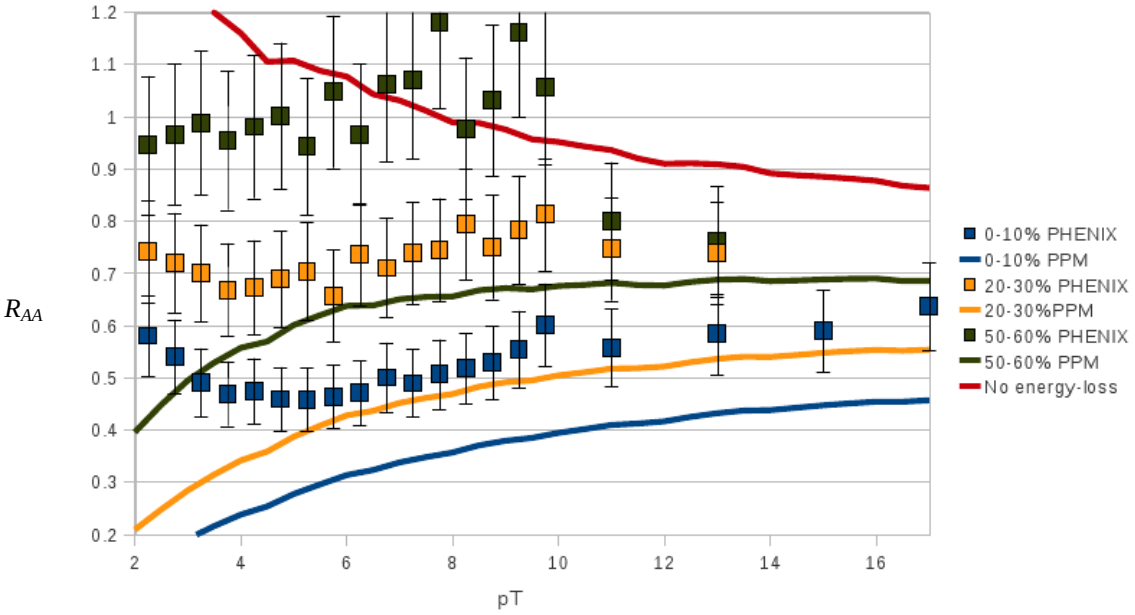

FIG.3.10. R_{AA} for Cu+Cu at 200 GeV. By using parameters c and λ as we did for Au+Au at 200 GeV clearly leads to an underestimate of experimental data.

There are several possible explanations for such a failure. One could be that the so-called Cronin Effect [16] becomes important for the smaller Cu+Cu system. This initial state effect is caused by multiple soft parton scatterings before the actual hard scattering that we study. As a consequence of such soft interactions, partons gain transverse momentum which causes a small

change in the initial jet distributions in the low pT region. Moreover, this effect is no longer seen in the high-pT region.

To correct this effect we multiply the initial jet distributions in PPM by

$$\left(1 + \frac{A^{1/3}C'}{pT^2}\right) \tag{5.1}$$

where the parameter C' is fixed to 3 GeV^2 so that it provides the best description of RHIC data on deuteron on gold (d+Au) collisions. The d+Au system has very little final state effects (due to small deuteron nucleus) and is therefore ideal to study initial state effects like the Cronin effect. FIG. 3.11 shows our calculation of R_{AA} for pions in d+Au collisions together with data from PHENIX.

We observe a small enhancement in the low pT region for Au+Au system (FIG 3.12) and no improvement on the fit overall. For the Cu+Cu system we see that suppression is reduced by 10% which overestimates experimental data still.

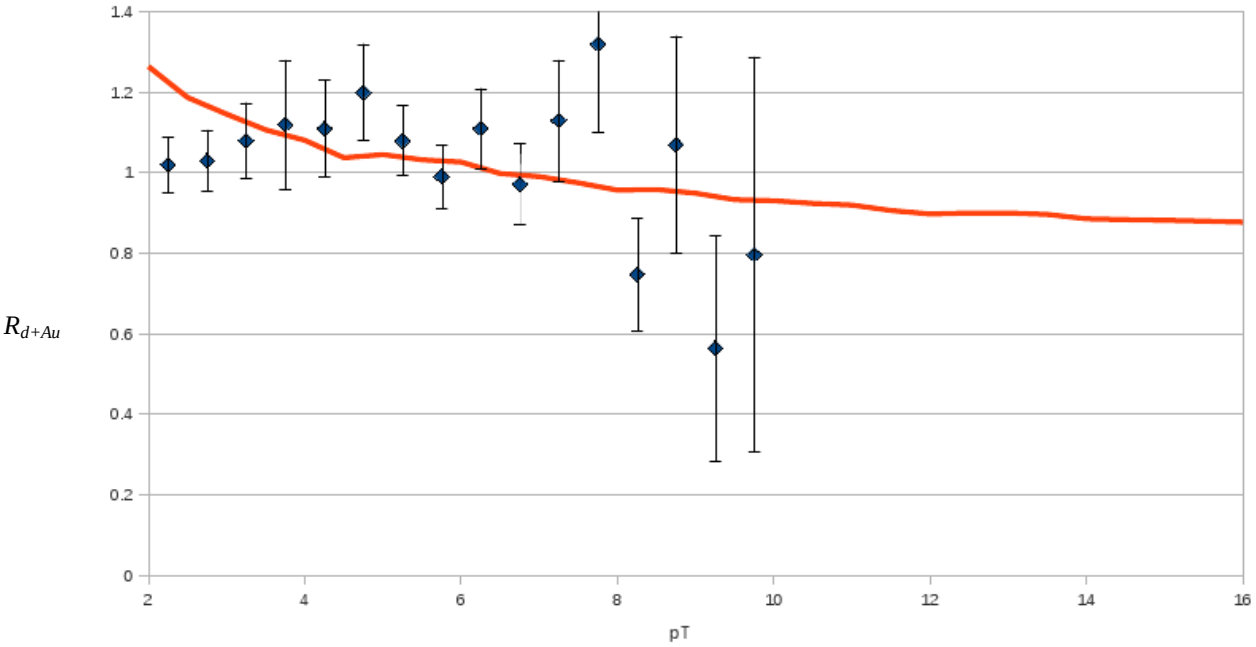

FIG. 3.11. Parameter C' fit to experimental R_{d+Au} results [17] (blue diamonds). C'=3 provided the best fit.

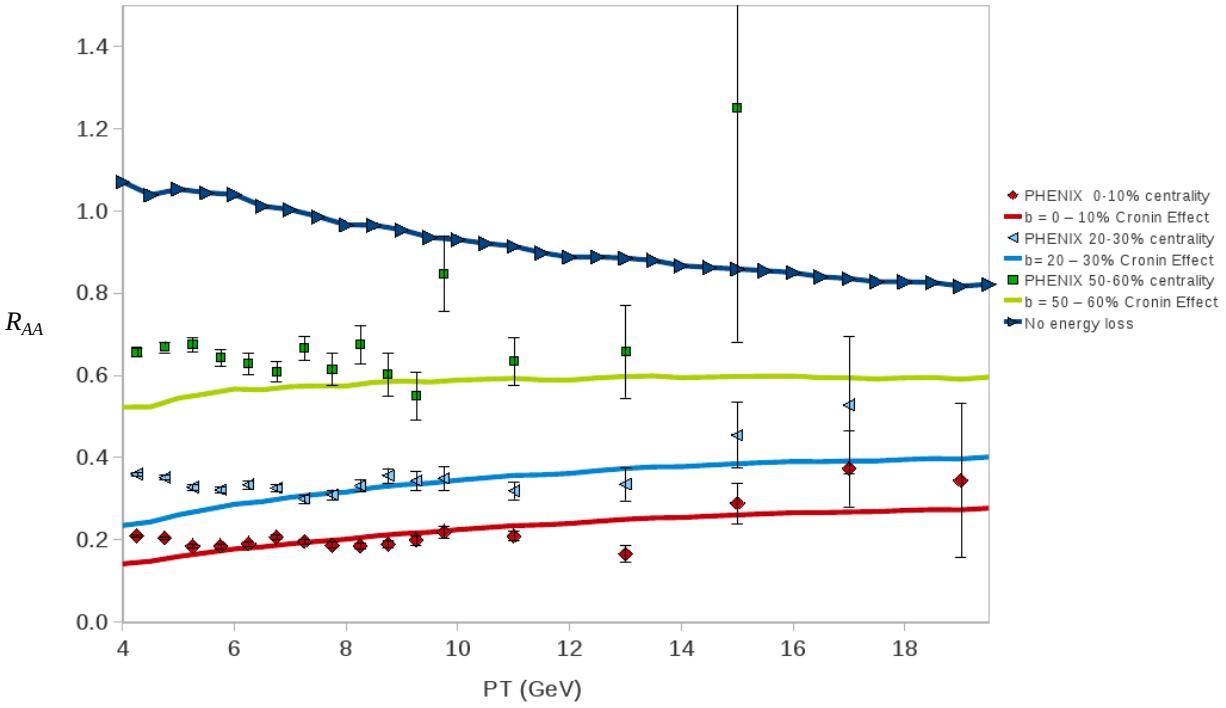

FIG. 3.12. Results for Au+Au at 200 GeV after implementation of Cronin Effect in jet fragmentation functions.

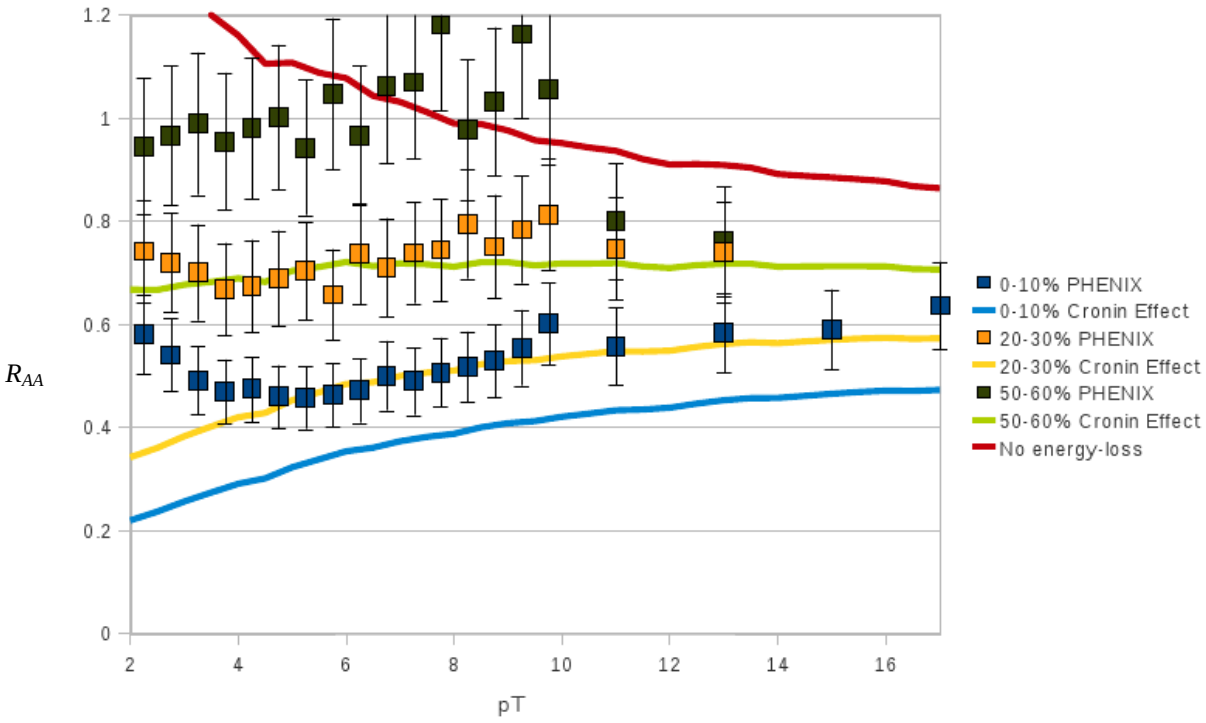

FIG. 3.13. Results for Cu+Cu at 200 GeV after implementation of Cronin Effect in jet fragmentation functions.

CHAPTER IV

DISCUSSION AND CONCLUSION

A systematic study of the dependence of energy loss of quarks and gluons on the local entropy density s in quark gluon plasma was conducted for this project with the purpose of obtaining a better description of R_{AA} and v_2. Along the way we improved and generalized the multi-purpose code PPM that calculates jet quenching observables in heavy ion collisions. Among the novel features we implemented are (i) initial jet distributions for Cu+Cu and d+Au collisions at RHIC energies, and Pb+Pb collisions at LHC energies; (ii) a parameterization of the Cronin effect which is important for small systems, like peripheral Cu+Cu collisions. The parameters were fit to existing pion data in d+Au collisions; (iii) binary collision- and participant-density maps for those systems calculated in a optical Glauber model. The corresponding code was written and is now available together with PPM; (iv) various profile functions which introduce different quenching strength $\hat{q}(s)$ around and above the critical entropy density, inspired by the shell model by Liao and Shuryak. All of these improvements to PPM will be used in current and future projects to simulate the interactions of jets with quark gluon plasma and to compare to experimental data with the goal to measure this interaction strength.

We tested the effects of shell-like quenching by implementing the model suggested by Liao and Shuryak. We recover their results qualitatively. We find that we can describe data on R_{AA} at RHIC energies reasonably well, and at the same time increase v_2, which had always been a problem for other energy loss models. Interestingly, at LHC we find a large spread of R_{AA}, generally increasing for more shell-like quenching. We observed larger v_2 at LHC for decreasing λ except for the most peripheral bins. This turning around of the qualitative behavior of v_2 could

be an easily accessible signature. Hence LHC data should be able to rule on the validity of enhanced quenching around the critical temperature. Our results can be understood by the fact that the shells become thinner by going to higher energies. Hence effective quenching starts to be limited to a very small space-time volume within the fireball at higher collision energies.

Contrary to the successful results when describing Gold systems at RHIC energies, we were unable to describe R_{AA} for the Copper system. Our results always underestimated experimental data by showing more suppression. We saw little improvement after implementing Initial State Effects in our calculations. A next step on the project would consider a more realistic model to simulate the nucleus, i.e. to replace the hard sphere approximation by a Woods-Saxon profile, and using appropriate linear combinations of binary collision- and participant densities.

One could also explore different beam energies for the Copper and Gold systems, such as 62.4 GeV (since experimental data is available) and check whether a shell-like model can describe R_{AA} better than conventional quenching profiles.

REFERENCES

[1] J. Adams, M. M. Aggarwal, Z. Ahammed, J. Amonett, B. D. Anderson *et al.,* Nucl.Phys. **A757,** 102-183 (2005).

[2] K. Adcox, S. S. Adler, S. Afanasiev, C. Aidala, N. N. Ajitanand *et al.*, Nucl.Phys. **A757**, 184-283 (2005).

[3] R. Baier, Y. L. Dokshitzer, A. H. Mueller, S. Peigne, D. Schiff, Nucl.Phys. **B484**, 265-282 (1997).

[4] C. Salgado and U. A. Wiedemann, Phys. Rev. D **68**, 014008 (2003).

[5] M. Gyulassy, P. Levai, I. Vitev, Nucl.Phys. **B594**, 371-419 (2001).

[6] A. Adare, S. Afanasiev, C. Aidala, N. N. Ajitanand, Y. Akiba *et al.*, Phys. Rev. Lett. **101**, 232301 (2008)

[7] M. Gyulassy and L. McLerran, Nucl.Phys. **A750**, 30-63 (2005).

[8] J. Liao and E. Shuryak, Phys. Rev. Lett. **102**, 202302 (2009).

[9] M. L. Miller, K. Reygers, S. J. Sanders, and P. Steinberg, Ann. Rev. Nucl. Part. Sci. **57**, 205 (2007), nucl-ex/0701025.

[10] R. Vogt, *Ultrarelativistic Heavy-Ion Collisions,* ("Elsevier", Radarweg 29, PO Box 211, 1000 AE Amsterdam, The Netherlands, 2007).

[11] J.F. Owens. Rev. Mod. Phys. **59**, 465 (1987).

[12] R.J. Fries, B. Muller, D.K. Srivastava. Phys. Rev. Lett. **90**, 132301 (2003).

[13] D.K. Srivastava, C. Gale, R.J. Fries. Phys.Rev. **C67**, 034903 (2003).

[14] R. Rodriguez, R.J. Fries, E. Ramirez-Homs. Phys. Rev. B **693**, 108-113 (2010).

[15] A. Adare *et al*., Phys. Rev. Lett. **101** 162301 (2008).

[16] R. J. Fries and C. Nonaka, Prog. Part. Nucl. Phys., *in press*, preprint arXiv:1012.1881 [nucl-th].

[17] S.S. Adler, S. Afanasiev, C. Aidala, N. N. Ajitanand, Y. Akiba *et al*., Phys. Rev. Lett. **91**, 072303 (2003).

CONTACT INFORMATION

Name:	Andrea Delgado
Professional Address:	Cyclotron Institute 3366 TAMU Texas A&M University College Station, TX 77843, USA
Email Address:	delgado.andrea.21@gmail.com
Education:	B.S., Physics, Texas A&M University, May 2013 Undergraduate Research Scholar